HHS Public Access

Author manuscript

Nat Med. Author manuscript; available in PMC 2019 August 18.

Published in final edited form as:

Nat Med. 2019 March ; 25(3): 419–422. doi:10.1038/s41591-019-0343-4.

Single-Dose CRISPR/Cas9 Therapy Extends Lifespan of Mice with Hutchinson-Gilford Progeria Syndrome

Ergin Beyret[1,*], **Hsin-Kai Liao**[1,*], **Mako Yamamoto**[1,2], **Reyna Hernandez-Benitez**[1], **Yunpeng Fu**[1], **Galina Erikson**[1], **Pradeep Reddy**[1], and **Juan Carlos Izpisua Belmonte**[1]

[1]Salk Institute for Biological Studies, 10010 N. Torrey Pines Rd., La Jolla, CA 92037

[2]Universidad Católica San Antonio de Murcia (UCAM), Campus de los Jerónimos, Nº 135, 12 Guadalupe 30107, Spain

Abstract

Hutchinson-Gilford Progeria Syndrome (HGPS) is a rare lethal genetic disorder characterized by symptoms reminiscent of accelerated aging. The major underlying genetic cause is a substitution mutation in the gene coding for lamin A, causing the production of a toxic isoform called progerin. Here we show that reduction of lamin A/progerin by a single dose systemic administration of AAV-delivered CRISPR/Cas9 components suppresses HGPS in a mouse model.

Laminopathies are degenerative disorders caused by mutations that affect proteins in the nuclear lamina[1]. The most severe forms manifest accelerated aging at the organismal level in correlation with premature degeneration of multiple tissues and organs[2]. Therefore, these diseases are attractive platforms to identify the molecular players of aging[3,4]. HGPS is one of the most severe forms of such diseases with an early onset, fast progression and assured lethality[5,6]. It is diagnosed shortly after birth, ensuing lethality at the average age of 14.6 years[7]. No cure currently exists and current treatments aim to alleviate the associated symptoms[8]. Although farnesyltransferase inhibitors (FTIs) have shown certain improvements and are now in clinical trials, this approach has limitations due to potential side effects of FTIs on other *CaaX* protein substrates, and because the effect of accumulated non-farnesylated progerin is unclear[9]. The majority of HGPS cases (~90%) results from *de novo* c. C1824T (p.Gly608Gly) mutation that increases the usage of a cryptic splicing site and production of a truncated lamin A called progerin[10–12]. The truncation removes an

Corresponding Author: Juan Carlos Izpisua Belmonte, belmonte@salk.edu.

*These authors contributed equally

Authors contributions

E.B., H.-K.L., and J.C.I.B. designed all experiments. E.B., H.-K.L., P.R., and J.C.I.B. prepared the figures and wrote the manuscript. E.B., H.-K.L., and Y.F. performed and/or analyzed *in vitro* experiments. E.B., H.-K.L., Y.F., M.Y., R.H.-B. and P.R. performed and/or analyzed *ex vivo* and *in vivo* experiments. G.E. performed the bioinformatics analyses.

Competing interests

The Authors declare no competing interests.

Reporting Summary

Further information on experimental design is available in the Life Sciences Reporting Summary linked to this article.

Data Availability

The accession number for the RNA-Seq data reported in this paper is NCBI GEO: GSE122865.

endoproteolytic cleavage site, preventing removal of the farnesylated tail. Consequently, the nuclear envelope deforms and cellular functions associated with it are impaired such as genomic stability, epigenetic regulation of gene expression, protein and energy metabolism, and nucleocytoplasmic transport[3,4,6,13]. Induction of the corresponding mutation in the mouse (Gly609Gly) induces similar phenotypes as in the human patients[14]. On the other hand, lamin A appears to be dispensable possibly due to compensation from its shorter isoform lamin C[14,15], and mice without lamin A live longer than wild-type mice[16], indicating that HGPS does not result from lack of lamin A but from the accumulation of progerin. Therefore, we reasoned that HGPS can be treated by CRISPR-Cas9-targeted disruption of lamin A/progerin.

Two guide RNAs (gRNAs: gLmna-1 and gLmna-2) for *Streptococcus pyogenes* Cas9 (SpCas9) targeting lamin A downstream of lamin C were designed to reduce lamin A/progerin without perturbing lamin C (Fig. 1a). The efficiency of the targeting was evaluated in fibroblasts isolated from HGPS; Cas9 mice that are heterozygous or homozygous for the progerin mutation and hemizygous for a constitutively active Cas9 transgene. Lentiviral delivery of the gRNAs individually or together efficiently down-regulated the levels of progerin and lamin A but not that of lamin C (Extended Data Fig. 1a,b). A gRNA with no target site on the genome (mock treatment) or the gRNAs without Cas9 did not elicit the effect indicating that down-regulation results from lamin A/progerin targeting by CRISPR/Cas9. Interestingly, high-throughput RNA-sequencing showed that either gRNA treatment correlated with downregulation of the RNA sequences downstream of lamin C suggesting the treatments caused lamin A/progerin-specific transcriptional interference or RNA destabilization (Extended Data Fig. 1c,d). A similar concurrent study[17] and a previous knock-in attempt in this region also concluded the same observation[15].

We next tested *in vivo* efficacy of the gRNAs in HGPS; Cas9 mice. Toward this end, individual gRNAs with a mCherry reporter were packaged into adeno-associated virus with serotype 9 (AAV9). Given that HGPS is a pediatric systemic disease, we systemically delivered the AAV9-gRNAs into the neonatal mice via facial vein injection (Fig. 1b). The two gRNAs were collectively administered for maximum efficiency (gLmna-1+ gLmna-2). mCherry reporter was detectable on day 4 post-injection in several organs, with liver displaying the highest expression (Fig. 1b,c and Extended Data Fig. 2a). The distribution of mCherry expression among the organs remained the same through the adulthood except for the intestine, which reduced to the background level (Extended Data Fig. 2b,c). Genomic DNA isolated from the organs of the adult mice injected with the gRNAs showed the highest level of editing in the liver in correlation with the protein levels (Fig. 1d,e and Extended Data Fig. 3). Consequently, the mice looked healthier and displayed an improved posture and body weight (Fig. 1f,g). Moreover, they were more active, which may be due to systemic physiological improvements and suppression of kyphosis (Videos 1, 2).

HGPS mice fail to thrive and gradually lose their body weight with age[14]. We monitored the body weight progression of the treated mice in comparison to the negative controls at two months old onwards. We observed that the treatment attenuated the weight loss (Fig. 2a). In parallel, the median survival rate increased by approximately 25% (Fig. 2b). The median survival rates for HGPS, HGPS/Cas9 and HGPS/Cas9 + two Lmna-gRNAs (g1&2) mice

were 16.7, 20.0, and 25.3 weeks, respectively. Given that HGPS is a progressive degenerative disorder, we analyzed the histology of the stomach and skin. These two organs undergo accelerated aging in HGPS mice[18] although human HGPS patients do not demonstrate a clinically impaired GI function. The treated mice analyzed displayed a qualitatively healthier glandular stomach, with the number of parietal cells comparable to the wild-type control while the mock-treated mice were notably deficient in the parietal cells. The treatment also suppressed epidermal thinning and dermal fat loss, two aging-associated skin conditions (Fig. 2c,d).

HGPS patients die mainly due to cardiovascular ailments similar to those seen in old age, therefore we analyzed the aortic arch and heart rate in HGPS mice. The treatment ameliorated the degeneration of vascular smooth muscle cells of the aortic arch compared to the control mice, as indicated by an increase in the number of nuclei in the medial layer (Extended Data Fig. 4a). Furthermore, although human HGPS patients do not demonstrate decreased heart rates, electrocardiographic (ECG) analysis revealed that the treatment attenuated the development of bradycardia observed in HGPS mice (Extended Data Fig. 4b).

Musculoskeletal system is one of the major systems impaired during aging and in HGPS, affecting the quality of life. We assessed musculoskeletal physiology by subjecting the mice to the grip strength test. The treated mice exhibited stronger forelimb and hindlimb grip in parallel to higher body weight. Given that there are no neurological deficits in HGPS, this observation indicates that the physiological decline of the skeletal muscle is suppressed (Fig. 2e and Extended Data Fig. 4c). We next evaluated the vitality of the mice by measuring their voluntary activity on running wheels. The treated mice retained their activity at a level similar to the wild-type controls (Fig. 2f,g). These results indicate that the lamin A/progerin targeting by CRISPR/Cas9 in HGPS mice improved their physiological functions in correlation with histological improvements, and extended their life expectancy.

Despite the increase in survival rate, the treated mice did not live up to the extent of wild-type mice. We observed a significant number of the treated mice died acutely unlike the progressive deterioration of untreated mice (Extended Data Fig. 5a). Before dying, they displayed acute weight loss and abdominal distension in parallel to difficulty in defecation (Extended Data Fig. 5b). The necropsy analyses indicated Megacolon/Megacaecum formation alongside hardened fecal matter, suggesting the reason for the lethality was the inability to discharge the excrements (Extended Data Fig. 5c). Given that lamin C-only transgenic mice are asymptomatic[14] whereas accumulation of farnesylated lamin A in the enteric nervous system induces the same symptoms[19], our observations suggest that the lethality might be due to the failure of the enteric nervous system of the colon caused by lack of the gene-editing (Fig. 1e). Untreated or mock-treated mice do not develop this phenotype, presumably because they die beforehand.

Altogether, our data show that CRISPR/Cas9-mediated lamin A/progerin reduction by a one-time intravenous therapy extends the health and lifespan of HGPS mice. For this study, we used transgenic mice that express *Streptococcus pyogenes* Cas9 and exogenously delivered the gRNAs as a proof of concept. Notably, the accompanying paper by Santiago-Fernández *et al.* demonstrates similar conclusions by intraperitoneal delivery of

Staphylococcus aureus Cas9 and gRNAs[17]. Thus, these two independent studies complement each other and reveal the potential use of CRISPR/Cas9 for the treatment of human HGPS patients. Although this strategy perturbs lamin A expression alongside progerin expression, knockout studies in the mouse show that mice that lack lamin A are viable[14–16] and even live longer than wild-type mice[16]. Given that HGPS is a lethal disorder, the extension of health and lifespan of patients by this approach offers an attractive mode of intervention. Interestingly, although we observed a modest therapeutic effect, this outcome correlated with the gene editing occurring mainly in the liver and minimally in other organs. A more wide-spectrum targeting including the colon or a combinatorial therapy with FTIs[9] may further serve to extend the life expectancy of HGPS patients.

Methods

All animal procedures were performed according to NIH guidelines and approved by the Committee on Animal Care at the Salk Institute.

Mouse Strains

The HGPS (Progeria) mouse model, carrying the progerin mutation G609G was generated by Carlos López-Otín at the University of Oviedo, Spain and kindly donated by Brian Kennedy of the Buck Institute. *Streptococcus pyogenes* Cas9 transgenic mice were obtained from the Jackson Laboratory (Stock No: 024858). HGPS mice are a mix of 129/Ola and C57BL/6 strains, and Cas9 mice are composed of 129, C57BL/6N, C57BL/6J and FVB/N backgrounds. Homozygous Progeria mice are infertile. The heterozygous mice were crossed with homozygous Cas9 mice to obtain the composite mice. The resulting trans-heterozygous mice were bred to obtain the homozygous Progeria mice that carried the Cas9 transgene (homo or hemizygous). Hemizygous Cas9 background was sufficient to reduce Lamin A/Progerin levels (Extended Data Fig. 3b). The heterozygous Progeria mice on the Cas9 background were used to maintain the line. Progeria mice are C57BL/6 strain. Cas9 mice are on a mixed background of 129, C57BL/6 and FVB/N. The mice were housed with a 12 hours light/dark cycle between 06:00 and 18:00 in a temperature-controlled room (22 ± 1°C) with free access to water valves and PicoLab Rodent Diet 20 (LabDiet, Catalogue No: 5053) provided on a wire bar lid. Mice that have lost more than 20% weight within a week or those that fell below 13 grams were provided moist food on the cage floor and a water bottle on the wire bar lid.

gRNA design

gLmna-1 was designed to target exon12 of mouse lamin A gene and encompasses the farnesylation site. gLmna-2 was designed to target the exon 11 within close proximity to the C>T HGPS mutation site. A gRNA with no target site on the genome was used as the mock gRNA control (gRNA Mock). gRNA sequences are listed in the Supplementary Table 1.

In vivo Gene Therapy of LMNA

Individual gRNAs were packaged into adeno-associated virus-9 (AAV9) vectors with the mCherry reporter according to the published protocol[20]. The expression of the gRNA and mCherry was driven by U6 and CAG promoters, respectively. A 1:1 mix of AAV9-gRNA1

and AAV9-gRNA2 was injected in 40μl PBS through the facial vein into the neonatal mice under hypothermia-induced anesthesia within 48 hours of birth (P0–2). Mice infected with AAV9s that carry mCherry alongside a gRNA with no target on the genome (Mock), or mCherry alone were used as the negative controls in addition to the untreated mice (no gRNA). Likewise, mice without the Cas9 transgene that underwent the AAV9-gRNA1&2 treatment served as “no Cas9” control. All the negative controls acted similarly. The injected titer ranged between 2×10^{10} - 1×10^{12} genomic copies (gc) per gRNA virus as determined by quantitative PCR: 2.6 X 1010 gc total (Fig. 1b), 2.6 X 1011 gc each (Fig. 1c), 1.2 X 1011 gc each (Fig. 1d), 4.8 X 1011 gc each (Fig. 1e), 6.2 X 1010 gc each (Fig. 1f), 6.2 X 1010 gc each (Fig. 2c). Detection of the mCherry signal was obtained with a Zeiss AxioZoom.V16 stereo microscope. The adult mice were perfused with PBS to wash out the blood before the organs were extracted for the imaging.

For the genomic DNA analysis in Figure 1d, organ pieces were first digested with (1mg/ml) Proteinase K in [100mM NaCl, 25mM EDTA, 10mM Tris pH8.0, 0.5% SDS] overnight at 55°C. The genomic DNA of the digests was isolated with phenol:chloroform:isoamyl alcohol (25:24:1) extraction followed by ethanol precipitation. The DNA was digested with HindIII (New England Biolabs, Catalogue No: R0104) to remove the untruncated lamin A in order to favor the PCR amplification of lamin A that underwent truncation by the simultaneous cut of gRNA1 and 2.

For the analysis of the protein levels by Western blotting, organs were isolated from the mice perfused with PBS, and homogenized in RIPA buffer [50mM Tris-HCl pH7.4, 150mM NaCl, 2mM EDTA, 1% NP-40, 0.1% SDS, 0.5% Sodium deoxycholate, 1mM PMSF and 1X Mini Protease inhibitor cocktail from Roche, Catalogue No: 11836153001). The genomic DNA was sheared by passing the lysate 10 times through a 23G needle. After 30 minutes of incubation on ice, the lysate was centrifuged at 13000 rcf at 4°C for 5 minutes to remove the debris. The protein concentration was estimated with BCA Protein Assay Kit (Pierce, Catalogue No: 23225 23227). Afterwards, the lysate was supplemented with 1mM DTT before running 5–25μg total protein on a 10–20% Novex WedgeWell Tris-Glycine gel (Catalogue No: XP1020-Box). Immunoblotting was performed on 0.45μm PVDF membranes. The membranes were blocked with 5% nonfat dry milk powder in TBST (Tris-buffered saline with 0.1% Tween 20) for 20 minutes at room temperature. Immunoblotting with the primary and secondary antibodies was performed for 2 hours at room temperature or overnight at 4°C. Detection was performed with SuperSignal West Pico or Femto Chemiluminescence Substrate Solution (ThermoFisher Scientific, Catalogue No: 34087 and 34095) on Hyblot CL autoradiography films (Catalogue No: E3018). The membranes were stripped by incubation in Restore Plus Stripping Buffer (ThermoFisher Scientific, Catalogue No: 46428) for 15 minutes at room temperature for re-probing. The western analyses were repeated at least twice with different samples (biological replicates). Full-length images of the immunoblots are provided in the Source Data, and quantification of the bands was performed by ImageJ software based on their integrated densities per area.

Ex vivo Gene Therapy of LMNA

Primary fibroblasts were isolated from the tail-tips of the adult mice of the indicated genotypes. 45000 cells were seeded per well of a 12 well plate the day before infecting them with the lentiviruses that express the mCherry reporter and the individual gRNA-Lmna 1 and 2 or the mock gRNA. mCherry-positive cells in the culture were visually counted under the microscope in at least 3 visual fields to estimate the infectivity. More than 65% infectivity was achieved. No selection or cell sorting was performed following the infection. The cells were passaged at least once before lysing for immunoblotting. They were processed similarly for western blotting as for the organ samples except Sodium deoxycholate was excluded from the RIPA buffer used for their lysis.

Histological Analyses

For the histological analyses, 19 weeks old mice of the indicated genotypes were perfused first with PBS then with 10% Formalin except, 4% paraformaldehyde (PFA) was used for the aortic arches instead of 10% Formalin. Whole organs were incubated in 10% Formalin at room temperature for 2 days except, the aortic arches were incubated in 4% PFA at 4°C for 16 hours. All the samples were stored in 70% ethanol at 4C° until paraffin embedding and sectioning. The sections were analyzed with Hematoxylin and Eosin staining. The areas of the medial layers and the number of nuclei they contained were calculated by using Image J 1.52c software. 3–5 mice from each condition were analyzed. The total number of the slide sections for the quantitation is indicated in the corresponding figure legends.

Physiological Analyses

For the analysis of the heart rate, mice were anesthetized with 2.5% isoflurane and monitored by using Power Lab data acquisition instrument (ADInstruments). Data processing and analysis were performed using LabChart8 (ADInstruments).

For the grip strength test, a tension meter measuring force in Newtons was stationed horizontally on a platform. The mouse was held by the tail and allowed to grip the tension bar with both paws before pulling away from the bar slowly until its grip was broken. 5 adult female mice and 5 adult male mice (16–18 weeks old) were used for each group (wild type, treated homozygous progeria and the negative control). Each mouse was subjected to the test 5 times each for its forelimb and hindlimb strength. Each estimate in the graph corresponds to 25 reads derived from 5 animals, measured 5 times.

The voluntary running wheel activity was recorded with the low-profile wireless running wheels connected to a computer via a wireless hub and analyzed with the included software (Med Associates Inc., Catalogue No: ENV-047). The animals were allowed to adapt to the wheels for at least 22 hours before integrating their activity into the estimates. The activities were integrated in only after the mice became adjusted to the wheels as determined by the activities showing circadian correlation (active at night). 1 of the 27 mice analyzed showed no interest on the running wheels as determined by small sporadic peaks of activity with no circadian correlation. This mouse was excluded from the study. All the mice that showed even low activity but with circadian correlation were included.

DNA Library Preparation and Deep Sequencing

Nested PCR was performed for the preparation of the DNA libraries for deep sequencing. The same Lmna F and Lmna R primers used in Figure 1d were also applied to this procedure. They were used for the first round of amplification of the nested-PCR procedure with limited PCR cycles using 100ng of genomic DNA. This PCR product was used for the second round of amplification of the nested-PCR procedure using primer pairs that contained adaptor sequences for deep sequencing (Lmna-1-adapter-F1 and Lmna-1-adaptor-R1 or Lmna-2-adapter-F3 and Lmna-2-adaptor-R3). The nested PCR product was purified using the QIAquick PCR Purification Kit (QIAGEN). This cleaned DNA library prep was subjected to deep sequencing as in the published protocol[19]. Primer sequences are listed in the Supplementary Table 1

RNA-Sequencing Analyses

Total RNA was isolated from the primary tail-tip fibroblasts of the indicated genotypes and treatments. gRNAs were delivered into the cultured cells by Lentiviral vectors. The cells were homogenized with Qiashredder spin columns (Qiagen) and processed with RNeasy Mini Kit (Qiagen) to isolate their total RNA. Quality assessment, library construction, and sequencing (stranded mRNA, HiSeq SE50) were performed by the Next Generation Sequencing Core of Helmsley Center for Genomic Medicine at Salk Institute. Bioinformatics analyses were performed by the Razavi Newman Integrative Genomics and Bioinformatics Core at Salk Institute. Sequenced reads were quality-tested using FASTQC and aligned to the mm10 mouse genome using the STAR[21] version 2.5.1b. Mapping was performed using the default parameters (up to 10 mismatches per read, and up to 9 multi-mapping locations per read). The normalized fragments per kilobase per million mapped reads (FPKM) were quantified across all annotated exons. The normalized read densities were visualized using the UCSC genome browser.

Antibodies

The following antibodies were used for immunoblotting at the indicated dilution: Anti-LAMIN A/C (N-18) 1:100 (SantaCruz, Catalogue No: sc6215), Anti-LAMIN A/C (E-1) 1:100 (SantaCruz, Catalogue No: sc376248), anti-β actin 1: 600 (SantaCruz, Catalogue No: sc47778), anti-α tubulin 1: 750 (Calbiochem, Catalogue No: CP06). HRP-conjugated secondary antibodies were anti-goat 1:500 (Novex, Catalogue No: A15909), anti-mouse 1:1000 (Cell Signaling, Catalogue No: 7076)

Statistical Analyses

Average (mean), standard error of the mean (SEM) and statistical significance were calculated by unpaired student's *t*-test (figure 2g), multiple *t*-test (figure 2a) or one-way ANOVA with Bonferroni correction (figures 1g and 2e) and log-rank (Mantel-Cox) test (figure 2b) using Microsoft Excel or GraphPad Prism. A p value of < 0.05 was considered significant ($*p < 0.05$, $**p < 0.01$, $***p < 0.001$), p values ≥ 0.05 were denoted as statistically not significant (n.s.)

Extended Data

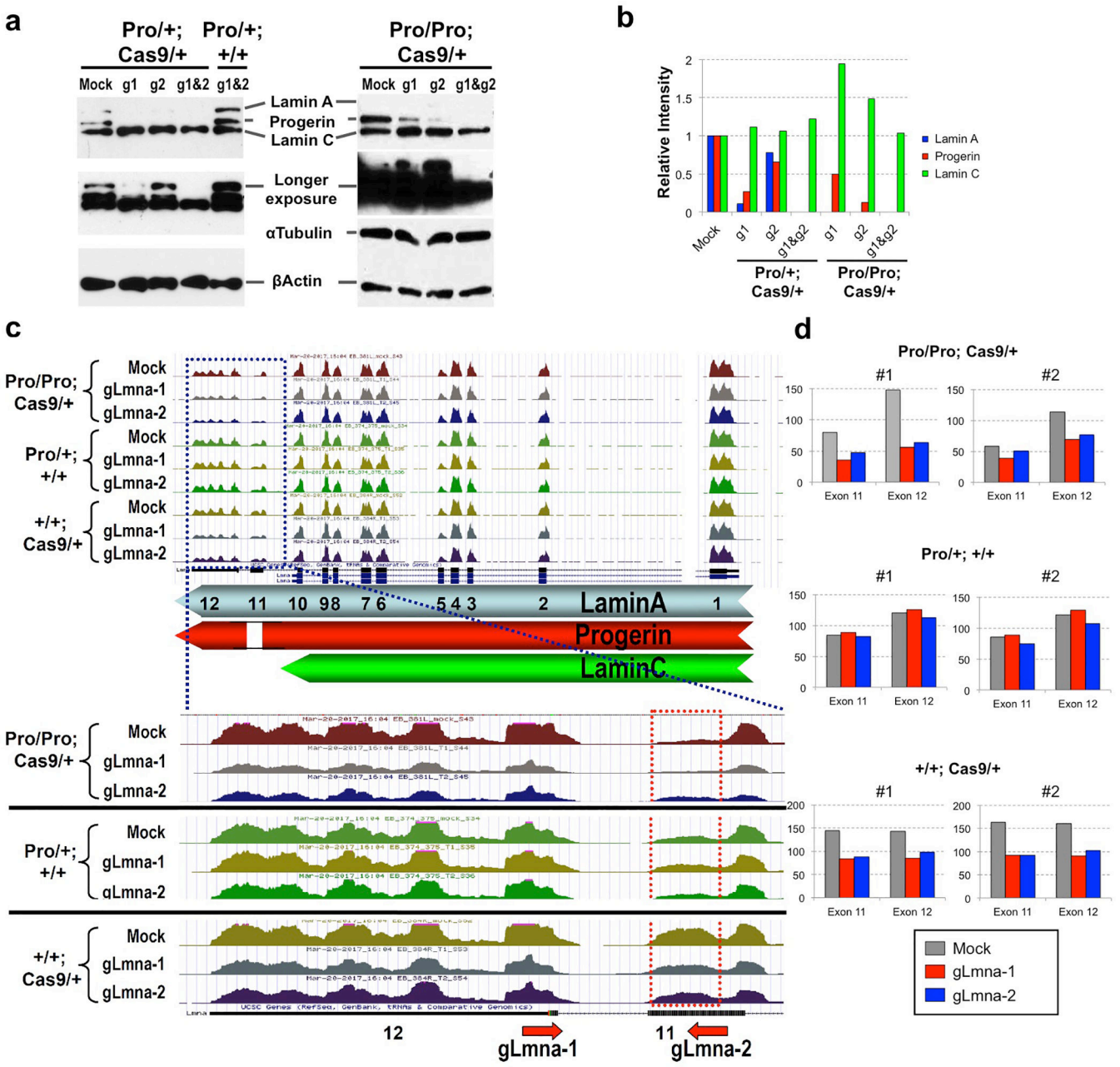

Extended Data Fig. 1|. Immunoblots and RNA sequencing of Lmna gRNA-treated fibroblasts of adult HGPS mice.

(a) Immunoblots of individual (g1 or g2) or multiplex (g1&2) gRNA-treated fibroblasts derived from adult HGPS (Pro); Cas9 mice. Fibroblasts derived from heterozygous (Pro/+) and homozygous (Pro/Pro) HGPS mice on heterozygous Cas9 (Cas9/+) background were treated with lentivirally-delivered gRNAs. No Cas9 (Pro/+; +/+) sample and mock-treatments were used as negative controls. Middle panels are longer exposures. aTubulin and pActin were used as loading controls, (**b**) Relative intensities of Lamin A, Progerin and Lamin C bands on the immunoblots. The intensity of each band was normalized by the pActin intensity and compared with the normalized mock control, (**c**) Custom tracks of the

RNA sequences identified with high- throughput sequencing. Magnified region corresponds to the squared area in blue. The red line denotes the truncated region in HGPS (Pro). Shown are the RNA samples derived from mouse fibroblasts of the indicated genotypes and treatments: + denotes wild type. Mock treatments and heterozygous HGPS mice without Cas9 (Pro/+; +/+) were used as negative controls. The arrows are not drawn to scale, (**d**) Quantification of the RNA sequencing analyses shows reduced transcription of the exons 11 and 12 in the Cas9-positive cells treated with the gRNAs relative to the mock-treated or Cas9-negative cells. Figures S1a–d are representatives of two independent replicates.

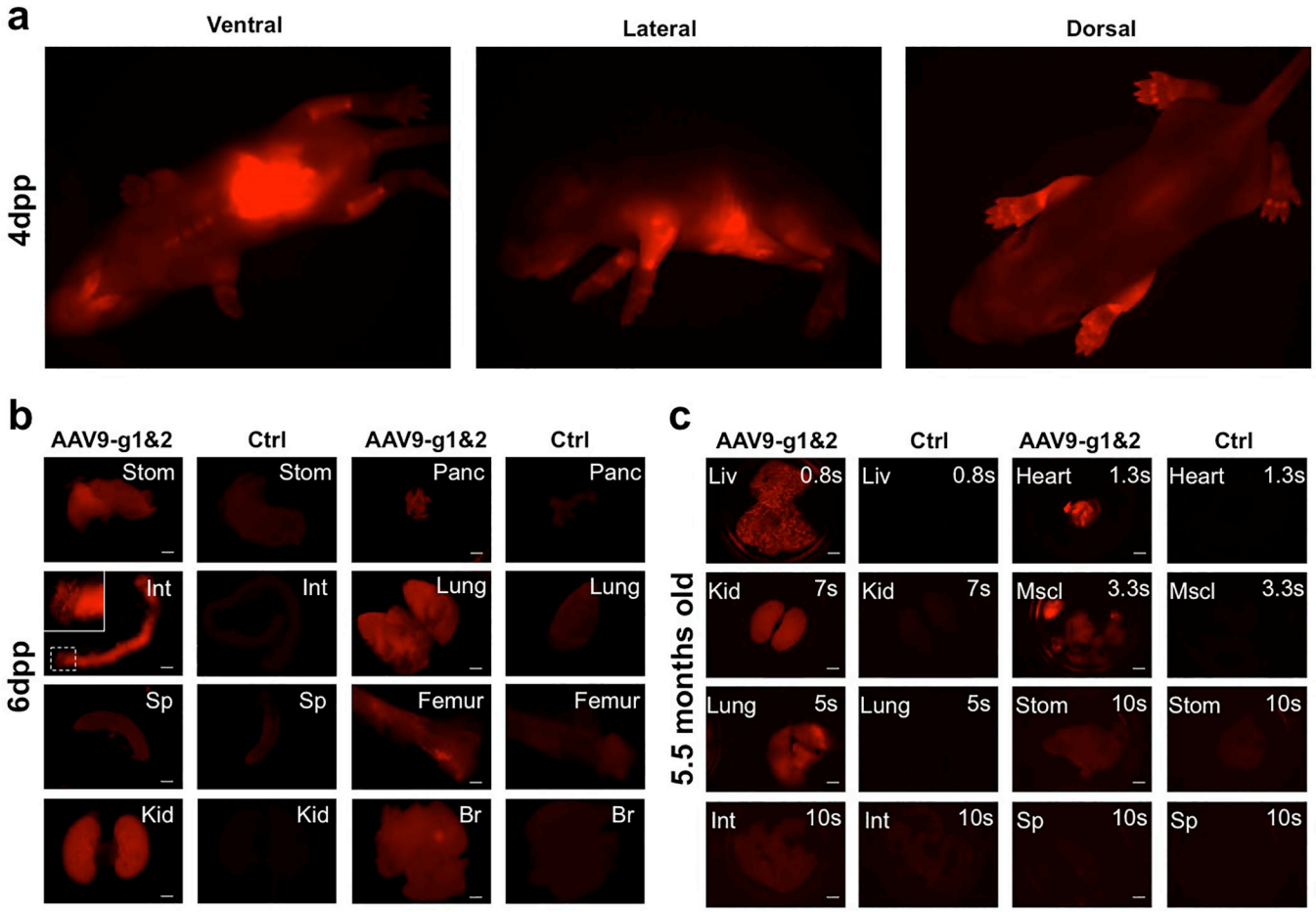

Extended Data Fig. 2|. Fluorescent images of Lmna gRNA injected mice.

(**a**) Whole body fluorescent images of a P4 (4dpp) mouse injected at PO with a 1:1 mix of gRNA1 and gRNA2 viral preps (each 1.29 × 1011 gc per viral prep), (**b**) Same organs as in Fig. 1c under individually adjusted exposure levels relative to their negative controls. The organs were harvested from a 6dpp mouse, 5 days post injection (DPI) at P1 (P1–5DPI). The inset corresponds to the squared area. Ctrl: No injection. Scale bar, 1.5 mm, except for Int 2mm. (**c**) Expression of the mCherry reporter in the adult (5.5 months post injection of a 1:1 mix of gRNA 1 and 2 viral preps) (1.3 X 1011 gc per viral prep). Figures S2a–c are representative replicates of at least two independent experiments. The numbers on the upper right corner denote the exposure time. Scale bar, 2.5 mm. Stom, Pane, Int, Sp, Kid, Br, Liv, Mscl: stomach, pancreas, intestine, spleen, kidney, brain, liver, muscle.

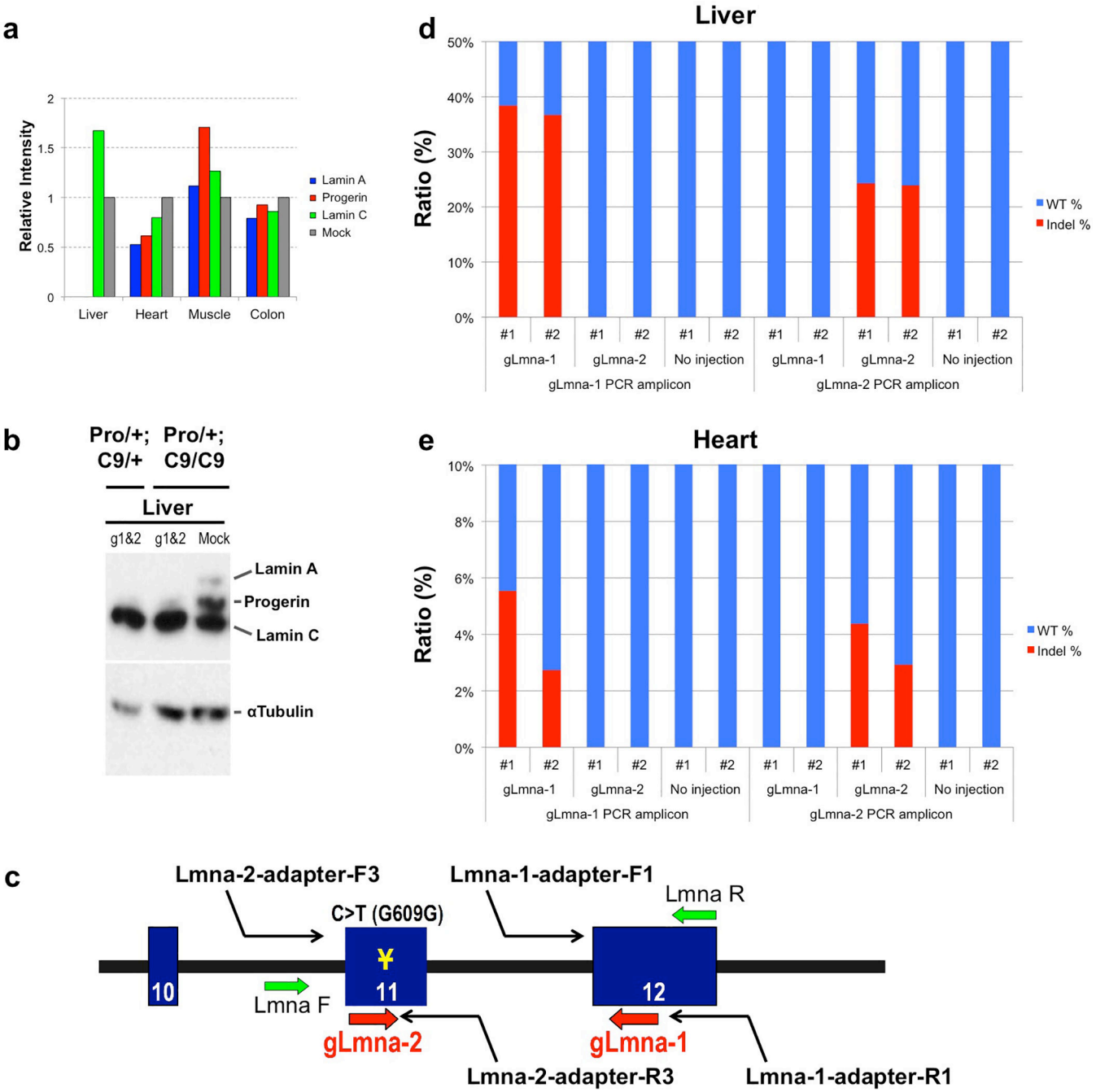

Extended Data Fig. 3|. Genomic DNA and protein analyses of Lmna gRNA treated mice.

(**a**) Relative intensities of Lamin A, Progerin and Lamin C bands on the immunoblot in Figure 1e. The intensity of each band was normalized by the aTubulin intensity and compared with the normalized mock control, (**b**) Immunoblot of adult liver lysate from g1&2-treated (5 X 10^{11} gc per viral prep) heterozygous HGPS (Pro/+) on hemizygous or homozygous Cas9 background shows single copy of Cas9 is sufficient. Figures S3a and S3b were representative replicate of two independent experiments with similar results. Figures S3a and S3b are representative replicates of two independent experiments with similar

results.(**c-e**) Deep sequencing was performed on liver and heart DNA to measure the level of *in vivo* indel formation by each gRNA. (**c**) Scheme of the deep sequencing strategy. gLmna-1 and gLmna-2 target sites are shown by red arrows. ¥ denotes the HGPS mutation. PCR amplicons of deep sequencing are indicated by black curved arrows. The locations of the primers (Lmna F and Lmna R) used for the first round of the nested PCR are shown by green arrows. Liver (**d**) and heart (**e**) DNA samples were collected from 2.5 months old Cas9 mice that had been injected at PO with either of the gRNA viruses (gLmna-1 or gLmna-2) (1.5×10^{11} gc viral prep), or with no virus. The gRNA treatments caused indels in their corresponding target sites and not in the target site of the other gRNA. No indels were detected in the “no injection” controls. Each treatment was evaluated in two independent *in vivo* experiments.

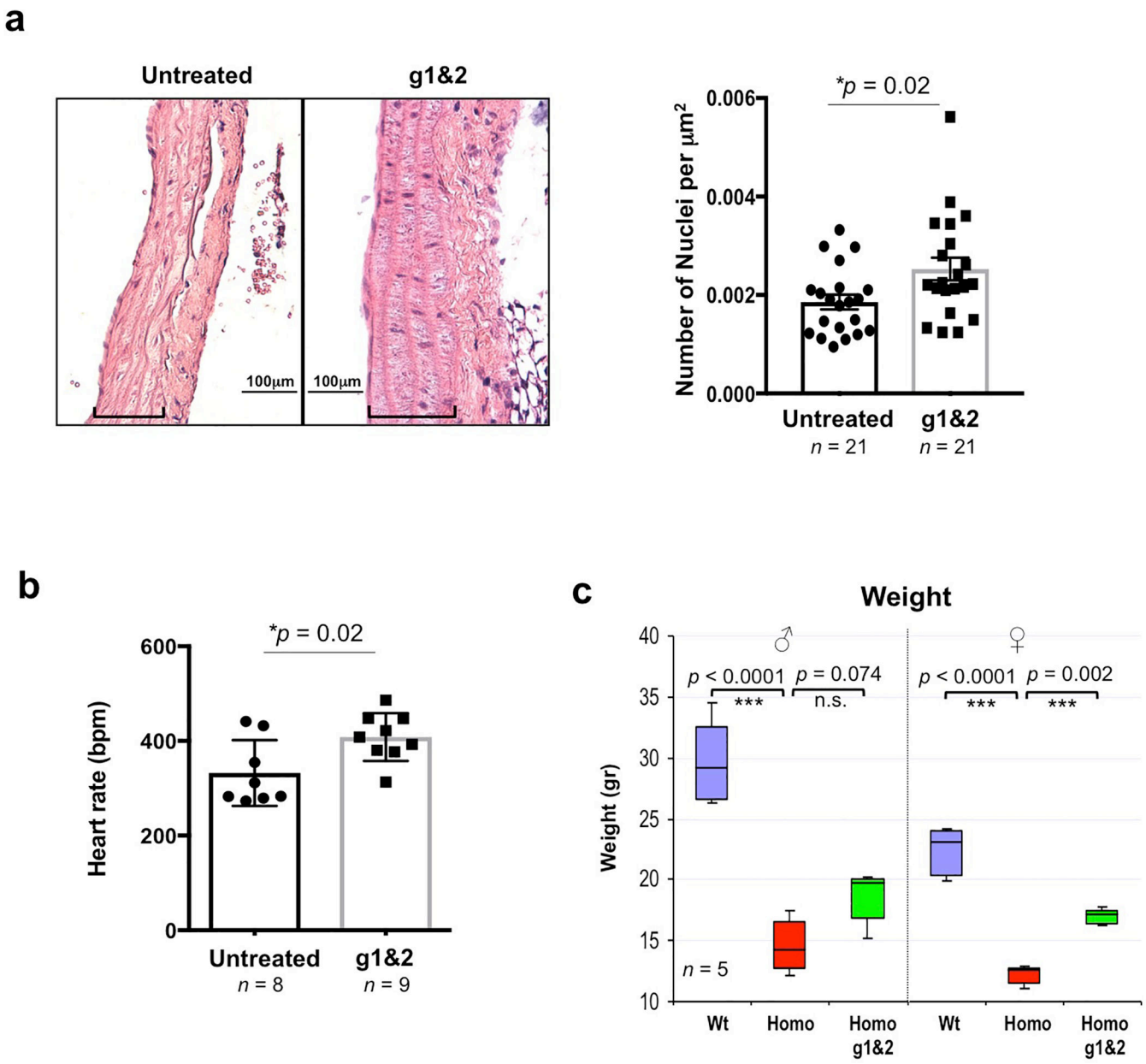

Extended Data Fig. 4|. Physiological analyses of Lmna gRNA treated mice.

(**a**) Histological analysis of the aortic arch of untreated and gRNA-treated (g1&2) HGPS; Cas9 mice that are 19 weeks old injected at PO with a 1:1 mix of gRNA1 and gRNA2 viral preps. The black bracket shows the medial layer of the aortic arch. Scale bar: 100 pm. The bar graph on the right shows the number of nuclei in the medial layer (n = 21 for each group), (**b**) Electrocardiographic (ECG) analysis of untreated and gRNA-treated (g1&2) HGPS; Cas9 mice (Untreated: n = 8; g1&2: n = 9). Heart rate is shown as beats per minute (bpm). Data are presented as mean ± SEM. P-values were calculated by unpaired Student's t-test in a) and b). (**c**) Body weight of the mice used for the grip strength test. Males and females are on the left and right, respectively. Cyan, red and green bars denote wild-type, negative control and treated mice. For each box plot, first and third quartiles denote 25th and

75th percentile and the black line represent the median. The whiskers represent the upper and lower limits of the data. Significance was determined by one-way ANOVA with Bonferroni correction.

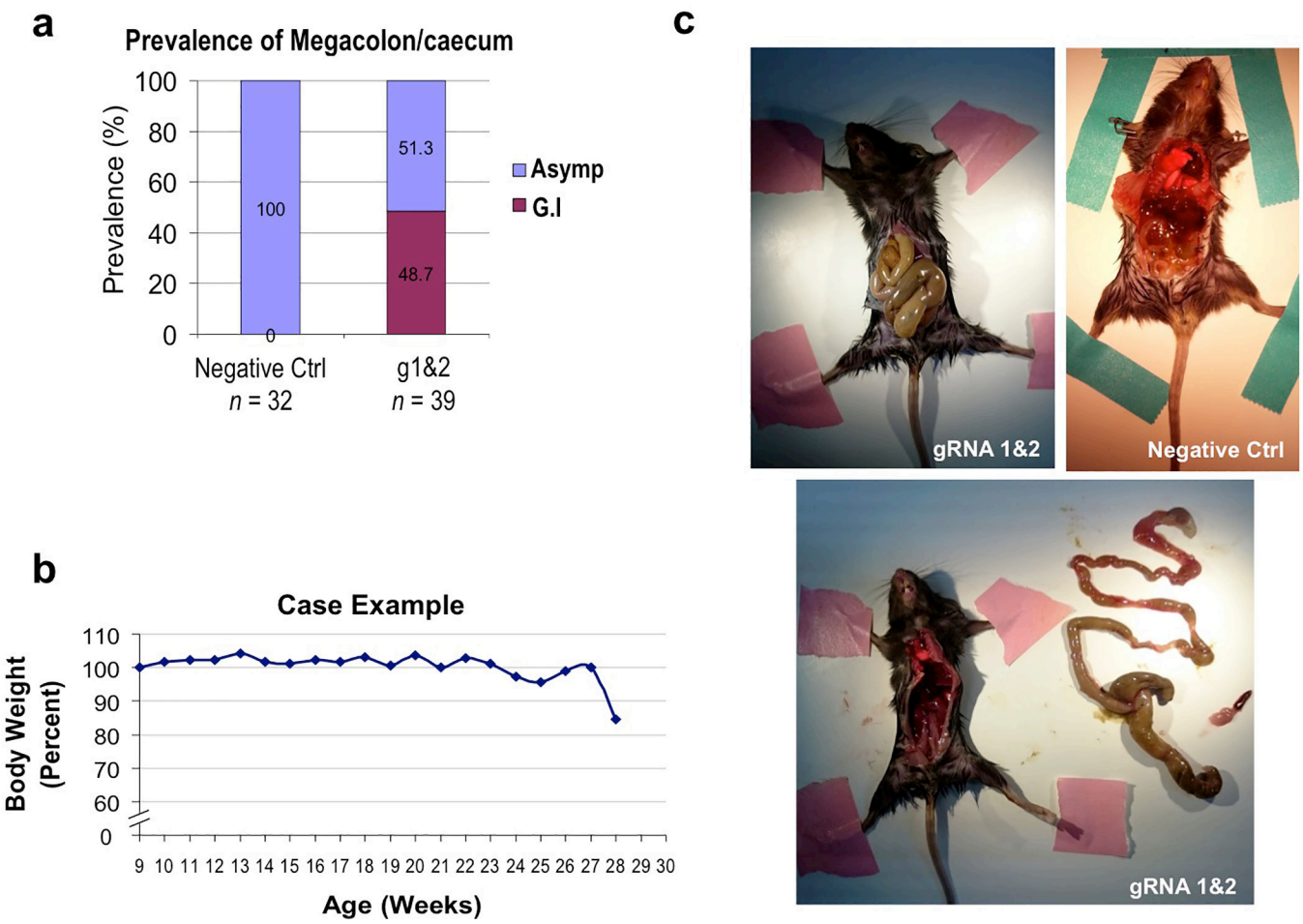

Extended Data Fig. 5|. Gastro-intestinal phenotype in the treated HGPS mice.

(**a**) Prevalence of Megacolon/ Megacaecum incidences among homozygous HGPS mice treated with gLmnal and 2 (g1&2) versus the negative controls. Asymp: Asymptomatic (no obvious gastrointestinal phenotype), G.I: gastrointestinal phenotype characterized with Megacolon/Megacaecum and inability to defecate. (**b**) Body weight progression of a representative g1&2-treated homozygous mouse that acutely died after 28 weeks, (**c**) Necropsy of a g1&2-treated homozygous mouse exhibiting Megacolon/Megacaecum (left and bottom photographs) unlike the negative control (right photograph).

Supplementary Material

Refer to Web version on PubMed Central for supplementary material.

Acknowledgements

We thank Alejandro Ocampo for discussions along the study, and May Schwarz for administrative support. We are grateful to Gencer Sancar and Ronald Evans Lab for providing the running wheel equipment. E. Beyret was partially funded by Catharina Foundation. P. Reddy was partially supported by the Muscular Dystrophy Association (MDA). G. Erikson was partially funded by NIH-NCI CCSG: P30 014195, and the Helmsley Trust. Work in the laboratory of J.C.I.B. was supported by The Progeria Research Foundation, Universidad Católica San Antonio de Murcia (UCAM), Fundacion Dr. Pedro Guillen, the G. Harold and Leila Y. Mathers Charitable Foundation, The Glenn Foundation and The Moxie Foundation.

References

1. Worman HJ, Fong LG, Muchir A & Young SG Laminopathies and the long strange trip from basic cell biology to therapy. J Clin Invest 119, 1825–36 (2009). [PubMed: 19587457]
2. Broers JL, Ramaekers FC, Bonne G, Yaou RB & Hutchison CJ Nuclear lamins: laminopathies and their role in premature ageing. Physiol Rev 86, 967–1008 (2006). [PubMed: 16816143]
3. Kubben N & Misteli T Shared molecular and cellular mechanisms of premature ageing and ageing-associated diseases. Nat Rev Mol Cell Biol 18, 595–609 (2017). [PubMed: 28792007]
4. Gordon LB, Rothman FG, Lopez-Otin C & Misteli T Progeria: a paradigm for translational medicine. Cell 156, 400–7 (2014). [PubMed: 24485450]
5. Ahmed MS, Ikram S, Bibi N & Mir A Hutchinson-Gilford Progeria Syndrome: A Premature Aging Disease. Mol Neurobiol. 55, 4417–4427 (2018) [PubMed: 28660486]
6. Gonzalo S, Kreienkamp R & Askjaer P Hutchinson-Gilford Progeria Syndrome: A premature aging disease caused by LMNA gene mutations. Ageing Res Rev 33, 18–29 (2017). [PubMed: 27374873]
7. Gordon LB et al. Impact of farnesylation inhibitors on survival in Hutchinson-Gilford progeria syndrome. Circulation 130, 27–34 (2014). [PubMed: 24795390]
8. Gordon LB, Brown WT & Collins FS Hutchinson-Gilford Progeria Syndrome. in GeneReviews® [Internet] (ed. Adam MP AH, Pagon RA, et al.) (University of Washington, Seattle; 1993–2018, Seattle (WA), 2003 Dec 12 [Updated 2015 Jan 8]).
9. Young SG, Yang SH, Davies BS, Jung HJ & Fong LG Targeting protein prenylation in progeria. Sci Transl Med 5, 171ps3 (2013).
10. Vidak S & Foisner R Molecular insights into the premature aging disease progeria. Histochem Cell Biol 145, 401–17 (2016). [PubMed: 26847180]
11. De Sandre-Giovannoli A et al. Lamin a truncation in Hutchinson-Gilford progeria. Science 300, 2055 (2003). [PubMed: 12702809]
12. Eriksson M et al. Recurrent de novo point mutations in lamin A cause Hutchinson-Gilford progeria syndrome. Nature 423, 293–8 (2003). [PubMed: 12714972]
13. Buchwalter A & Hetzer MW Nucleolar expansion and elevated protein translation in premature aging. Nat Commun 8, 328 (2017). [PubMed: 28855503]
14. Osorio FG et al. Splicing-directed therapy in a new mouse model of human accelerated aging. Sci Transl Med 3, 106ra107 (2011).
15. Fong LG et al. Prelamin A and lamin A appear to be dispensable in the nuclear lamina. J Clin Invest 116, 743–52 (2006). [PubMed: 16511604]
16. Lopez-Mejia IC et al. Antagonistic functions of LMNA isoforms in energy expenditure and lifespan. EMBO Rep 15, 529–39 (2014). [PubMed: 24639560]
17. Olaya Santiago-Fernández FGO, Quesada Víctor, Rodríguez Francisco, Basso Sammy, Maeso Daniel, Rolas Loïc, Barkaway Anna Louise, Nourshargh Sussan, Freije José M. P., López-Otín Carlos. Nat Medicine, In Press.
18. Ocampo A et al. In Vivo Amelioration of Age-Associated Hallmarks by Partial Reprogramming. Cell 167, 1719–1733 e12 (2016). [PubMed: 27984723]
19. Yang SH et al. Mice that express farnesylated versions of prelamin A in neurons develop achalasia. Hum Mol Genet 24, 2826–40 (2015). [PubMed: 25652409]
20. Liao HK et al. In Vivo Target Gene Activation via CRISPR/Cas9-Mediated Trans-epigenetic Modulation. Cell 171, 1495–1507 e15 (2017). [PubMed: 29224783]
21. Dobin A et al. STAR: ultrafast universal RNA-seq aligner. Bioinformatics 29, 15–21 (2013). [PubMed: 23104886]

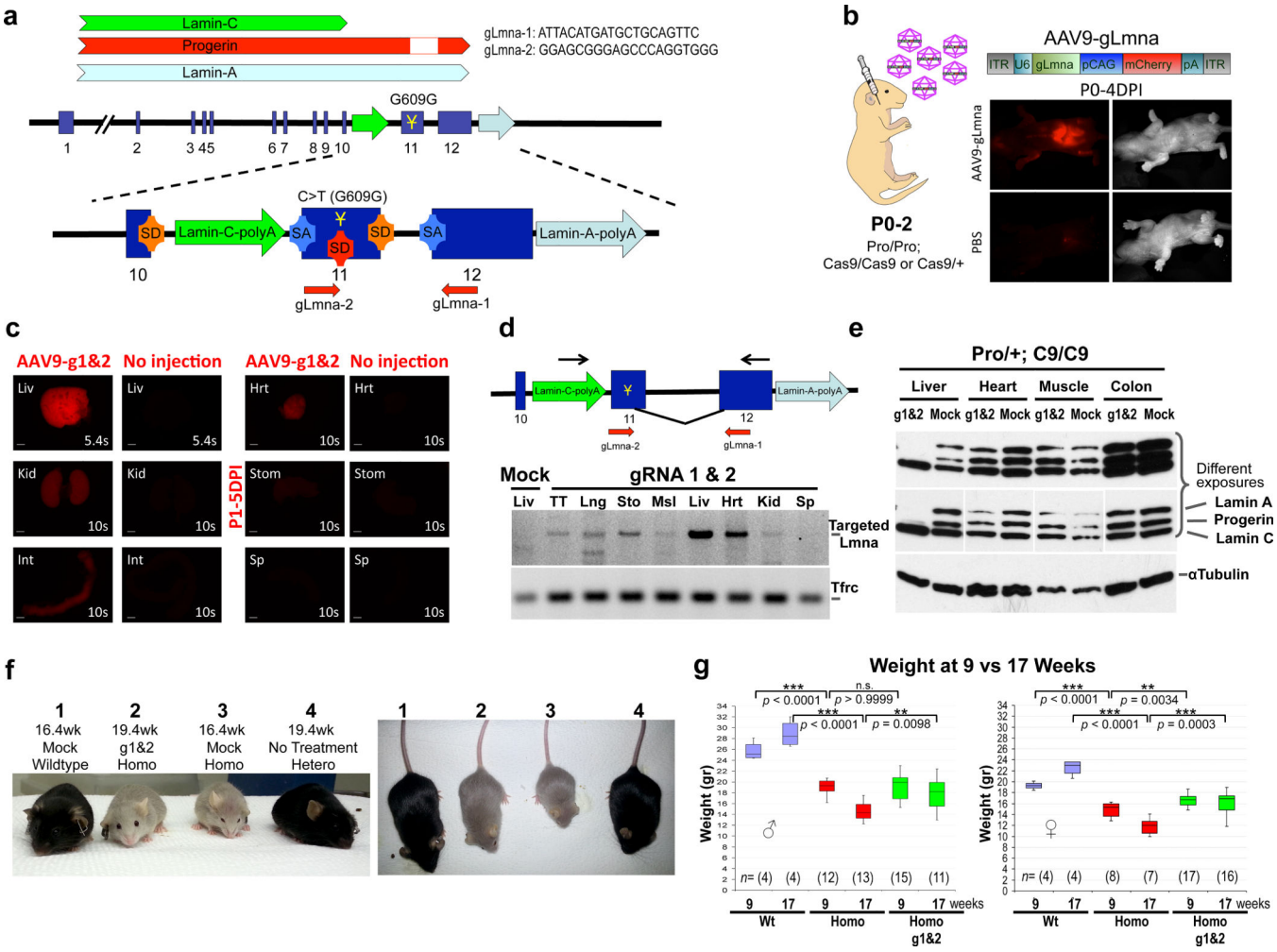

Figure 1: Targeted disruption of lamin A and progerin by CRISPR/Cas9.

a, Scheme of lamin A/progerin targeting by CRISPR/Cas9. gLmna-1 targets upstream of the farnesylation site, gLmna-2 recognizes mutation and wildtype site (Ɣ). SA/D: Splice Activator/Donor site. **b**, The *in vivo* gene therapy scheme. AAV9-mCherry-gLmna was injected into 0-to-2-day-old mice (P0–2). Upper panel shows the mCherry signal 4 days post-injection (DPI) into a P0 mouse (P0–4DPI) versus the PBS-injected control (lower panel). **c**, Expression of the mCherry reporter in different organs at 6dpp (days postpartum, P1–5DPI). The numbers at the lower right corners denote the exposure time in seconds. Scale bar, 2 mm. **d**, Efficiency of the lamin A/progerin targeting. When the two gRNAs act simultaneously, the region between them is deleted and the re-ligated ends can be detected by PCR. Black arrows denote the location of the primers. Tfrc: positive control for PCR. Mock: A gRNA with no target site on the genome. **e**, Immunoblots of adult organ lysates from heterozygous HGPS (Pro/+) mice on homozygous Cas9 (C9/C9) background treated with g1&2 versus mock-treated to evaluate lamin A/C/progerin levels. Middle panel corresponds to the uppermost blot under different exposures. α Tubulin: loading control (Fig. 1b–e are representative replicates of at least two independent experiments). **f**, Gross morphology of the mice. Shown are 16.4 weeks (wk) old mock-treated wild-type and

homozygous (homo) female siblings next to 19.4 weeks old heterozygous (hetero) and g1&2-treated homozygous female siblings (Also displayed in the videos 1 and 2). The difference in the morphology is although the mock-treated control is 3 weeks younger. **g**, Body weight comparison between 9 and 17 weeks with the males depicted on the left, and the females on the right. For each box plot, first and third quartiles denote 25th and 75th percentile and the black line represent the median. The whiskers represent the upper and lower limits of the data. Significance was determined by one-way ANOVA with Bonferroni correction. Liv, TT, Hrt, Lng, Kid, Stom, Msl, Int, Sp: liver, tail-tip, heart, lung, kidney, stomach, muscle, intestine, spleen.

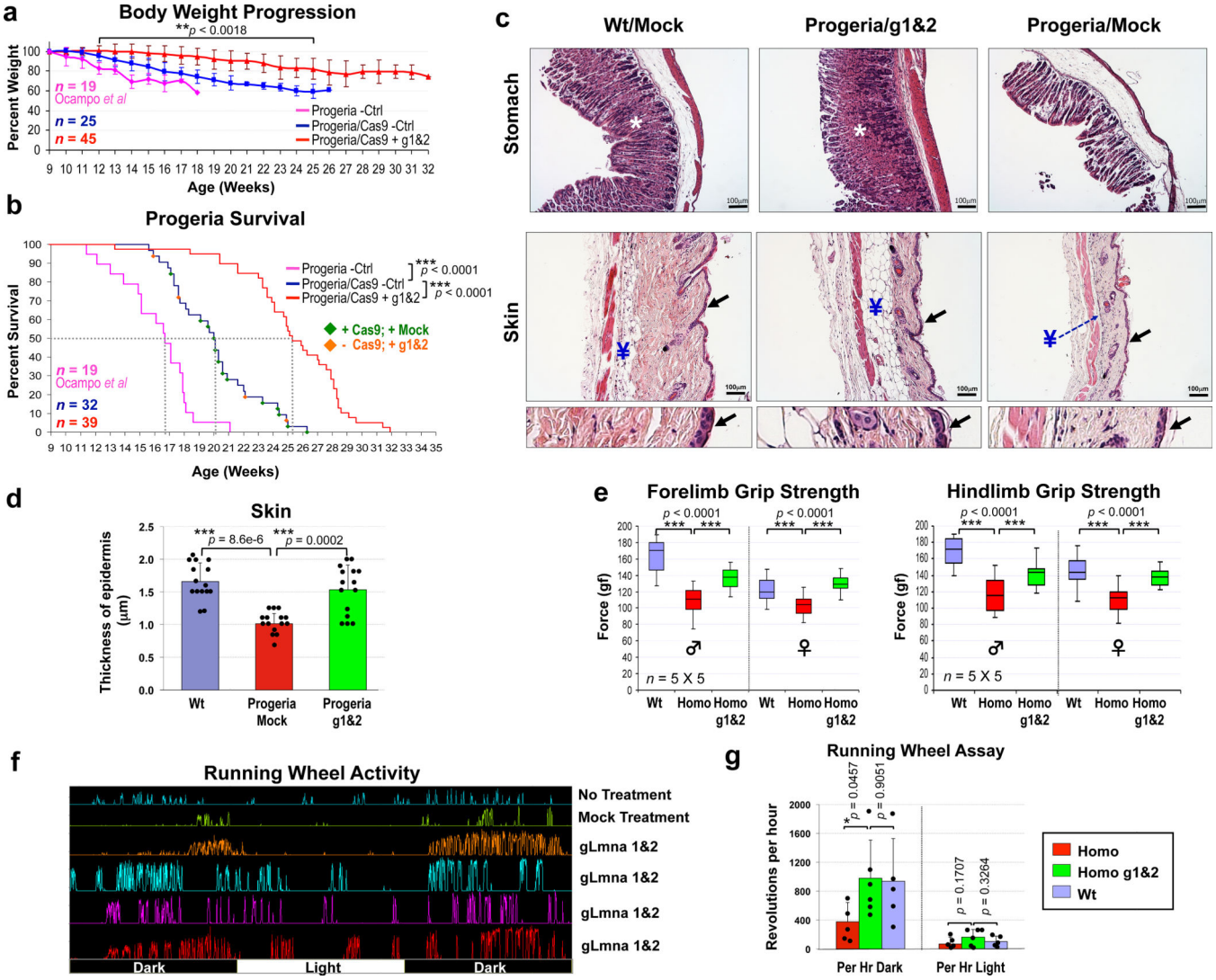

Figure 2: CRISPR/Cas9-induced reduction of lamin A/progerin extends the health and lifespan of the HGPS mice.

a, Body weight and **b**, survival rate through time. Magenta line denotes untreated homozygous HGPS (Progeria) mice analyzed in the paper of A. Ocampo *et al*[18]. The mice depicted in blue and red lines are a cross between HGPS and Cas9 transgenic mice (Progeria/Cas9 mice). They are homozygous for HGPS and carry at least one copy of the Cas9 transgene (hemizygous or homozygous). Blue line denotes untreated mice. Except for green and orange diamonds on the blue line in (**b**) denote mock-treated and gRNA-only negative controls, respectively. Red line denotes g1&2-treated mice. The sample size (*n*) indicates the initial number of mice at week 9 in Fig. 2a and 2b. Shown are mean values ± standard deviations. Multiple t-tests and log rank (Mantel Cox) test were used for body weight and survival curves, respectively. Although introduction of Cas9 alone seems to increase the survival rate, this may result from the different strain backgrounds following crossing with Cas9 mice. **c**, Histological analyses of the stomach (upper panel) and skin (lower panel) derived from 19 weeks old g1&2-treated versus mock-treated homozygous mice next to mock-treated wild-type (Wt). The arrows and asterisks denote epidermis of the

skin and parietal cells of the stomach, respectively. Ɣ: dermal fat. The figures at the bottom are the enlarged views of the epidermal regions pointed by the arrows. The images are representative replicates of two independent experiments with similar results. Scale bar, 100 μm. **d**, Measurement of the epidermal thickness (n = 15 sections per group from 3 biologically independent samples). Shown are mean, SEM and statistical significance were calculated by unpaired student's t-test. **e**, Grip strength test. Left and right panels depict forelimb and hindlimb grip strength of adult mice (16–18 weeks old), respectively. Each estimate corresponds to 25 reads derived from 5 animals, measured 5 times. For each box plot, first and third quartiles denote 25th and 75th percentile and the black line represent the median. The whiskers represent the upper and lower limits of the data. Significance was determined by one-way ANOVA with Bonferroni correction. **f**, Representative graph of the running wheel activities. Shown are the activities of untreated or mock-treated versus g1&2-treated homozygous mice. All treated mice were 17 weeks old and control mice were 4 weeks younger. **g**, Quantitation of the running wheel activities. Mice tested were between 10–18 weeks old. Blue bars denote wild-type mice (n=5), red and green bars denote control (n=5) and g1&g2-treated (n=6) homozygous HGPS mice, respectively. Shown are mean values ± standard deviations and significance according to unpaired t-test.